Fuzzy-Bayes Fault Isolator Design for BLDC Motor Fault Diagnosis

Suhk-Hoon Suh

Abstract: To improve fault isolation performance of the Bayes isolator, this paper proposes the Fuzzy-Bayes isolator, which uses the Fuzzy-Bayes classifier as a fault isolator. The Fuzzy-Bayes classifier is composed of the Bayes classifier and weighting factor, which is determined by fuzzy inference logic. The Mahalanobis distance derivative is mapped to the weighting factor by fuzzy inference logic. The Fuzzy-Bayes fault isolator is designed for the BLDC motor fault diagnosis system. Fault isolation performance is evaluated by the experiments. The research results indicate that the Fuzzy-Bayes fault isolator improves fault isolation performance and that it can reduce the transition region chattering that is occurred when the fault is injected. In the experiment, chattering is reduced by about half that of the Bayes classifier's.

Keywords: Bayes isolator, fault diagnosis, Fuzzy-Bayes isolator, transition region chattering.

1. INTRODUCTION

The purpose of Fault Detection and Isolation (FDI) is to detect a fault as it occurs and to identify the component in order to perform appropriate maintenance before critical system malfunctions occur. FDI can be applied to plants, which demand a high degree of system reliability such as power plants and avionics systems.

A brushless DC (BLDC) motor is essentially an ac motor in every respect. However, the performance of the BLDC motor is found to be equal or superior to the efficiency of the high-performance dc servo motor. In the BLDC motor, the commutation of the coil is carried out by an electronic inverter. This eliminates the brush sparking of the conventional DC motor, which reduces the insulation resistance to an unacceptable limit. Nevertheless, a BLDC motor can also fail. In particular, overload and overheating can damage the stator coil, thus resulting in decreased performance. Moreover, necessary sensors for position detection, e.g., hall sensors, can also fail as damaged or broken bearings may result in increased friction. In the closed-loop operation of servo systems, these faults often remain hidden by feedback. Only if the entire device fails, i.e., the motor stops turning, does the malfunction becomes visible. Therefore, it is desirable to detect an incipient fault as early as possible to perform maintenance before failure of the device occurs [1]. Xiang-Qun *et al.* [2] discussed DC motor fault detection and diagnosis by parameter estimation and neural network. Where the electromechanical parameters of the motor can be obtained from the estimated model parameters, the relative changes of electromechanical parameters are used to detect motor faults. The neural network is used to isolate faults based on the patterns of parameter changes. Moseler *et al.* [3] presented a real time fault detection method for a BLDC motor driving a mechanical actuation system in which they drive a mathematical model based on the bridge supply voltage, current and rotor velocity.

This paper proposes the Fuzzy-Bayes classifier, which consists of the Bayes classifier, and weighing factor. Because the Bayes classifier has optimal classification performance, the Bayes classifier is a representative algorithm of pattern classification. And it is used for fault diagnosis of the process rig [4], and BLDC motor [5]. The Bayes classifier depends on probability density functions, and a priori probabilities. The Mahalanobis distance derivative is mapped according to weighting factor by fuzzy inference logic. This means that the feature data dynamics are included in the classifier. Therefore, the classifier can be more insensitive to noise. The Fuzzy-Bayes classifier is designed for the BLDC motor fault diagnosis system, which is divided into a fault detection part, and a fault isolation part. The fault detection element detects fault symptoms by estimating parameters. Then, the fault symptoms are classified into faults by the fault isolator. By including the weighting factor, performance of the Bayes isolator is improved. The experiment results support it.

Section 2 describes the Bayes classifier, and proposes the Fuzzy-Bayes classifier. The BLDC motor fault diagnosis system is presented in Section 3. In Section 4, the BLDC motor fault diagnosis results

Manuscript received December 28, 2003; revised May 2, 2004; accepted July 1, 2004. Recommended by Editorial Board member Jietae Lee under the direction of Editor Jin Bae Park.

Suhk-Hoon Suh is with the R&D Dept., Next Instrument, 869 Jangji-ri, Dongtan-myeon, Hwaseong-Si, Kyunggi-Do 445-812, Korea (e-mail: shsuh@nextin.co.kr).

according to the Fuzzy-Bayes classifier are compared to that of the Bayes classifier. The conclusions are described in Section 5.

2. FUZZY-BAYES CLASSIFIER

2.1. Bayes classifier

The fundamental principle of the Bayes classifier is the Bayes rule, shown in (1)

$$P(\omega_i \mid x) = \frac{p(x \mid \omega_i)P(\omega_i)}{\sum_{j=1}^{c} p(x \mid \omega_j)P(\omega_j)}. \quad (1)$$

The Bayes rule indicates how the information of known probability density functions, $p(x|\omega_i)$, and a priori probabilities, $P(\omega_i)$, can be used to calculate the a posteriori probability, $P(\omega_i|x)$. The minimum-error-rate classification can be achieved by use of the Bayes discriminant functions [6],

$$g_i(x) = \ln P(x|\omega_i) + \ln P(\omega_i), \text{ where } i=1, \cdots, c, \quad (2)$$

and this expression can be readily evaluated if the densities $p(x|\omega_i)$ are normal distribution - that is, if $p(x|\omega_i) \sim N(\mu_i, \Sigma_i)$. In this case, we have

$$g_i(x) = -\frac{1}{2}(x-\mu_i)^t \sum\nolimits_i^{-1}(x-\mu_i) - \frac{d}{2}\ln 2\pi - \frac{1}{2}\ln|\sum\nolimits_i| + \ln P(\omega_i). \quad (3)$$

All the necessary information of each class and feature cluster is contained in the mean vector and covariance matrix. The center of each cluster is determined by the mean vector and the shape of the cluster by the covariance matrix. The quantity $r^2 = (x-\mu_i)^t \sum_i^{-1}(x-\mu_i)$ from (3) is often called the Mahalanobis distance from observation x to the center of the cluster μ.

2.2. Fuzzy-Bayes classifier

Equation (4) expresses the decision rule of the Fuzzy-Bayes classifier.

If $f_i > f_j$,

Decide ω_i if $f_i \cdot P(\omega_i \mid x) > f_j \cdot P(\omega_j \mid x)$;

otherwise decide ω_j.

where,

$$f_i = \begin{cases} 1 & u_1 \geq bound_2 \\ 0 \leq f_i \leq 1 & bound_1 < u_1 < bound_2 \\ 0 & u_1 \leq bound_1 \end{cases} \quad (4)$$

The $bound_1$, and $bound_2$ present the minimum and maximum value of the input u_1. The input u_1 is mapped to weighting factor, f_i, by the fuzzy inference logic. The posteriori probability, $P(\omega_i|x)$, can be determined by the Bayes rule. Therefore, the Fuzzy-Bayes classifier is composed of the Bayes classifier and weighting factor. The proposed discriminant function is presented in (5),

$$g_i(x) = -\frac{1}{2}(x-\mu_i)^t \sum\nolimits_i^{-1}(x-\mu_i) - \frac{d}{2}\ln 2\pi - \frac{1}{2}\ln|\sum\nolimits_i| + \ln P(\omega_i) + f_i(t). \quad (5)$$

In this paper, Mahalanobis distance derivative is selected as an input u_1. Thus, the feature data dynamic characteristic is involved in the weighting factor. The classification algorithm of the Fuzzy-Bayes classifier is depicted in Fig. 1.

If the input u_1 is greater or lower than bound_2 or bound_1, weighting factor, $f_i(t)$, is mapped to 1 or 0. If the u_1 is located between the lower and upper bound, the weighting factor is determined by fuzzy inference logic. To determine the weighting factor, two rules fuzzy model is supposed, and the rules are

$$\text{IF } u_1 \text{ is } \tilde{A}^1 \text{ THEN } b_1,$$
$$\text{IF } u_1 \text{ is } \tilde{A}^2 \text{ THEN } b_2, \quad (6)$$

where, $\tilde{A}^j$ denotes the j-th linguistic value and b_i =

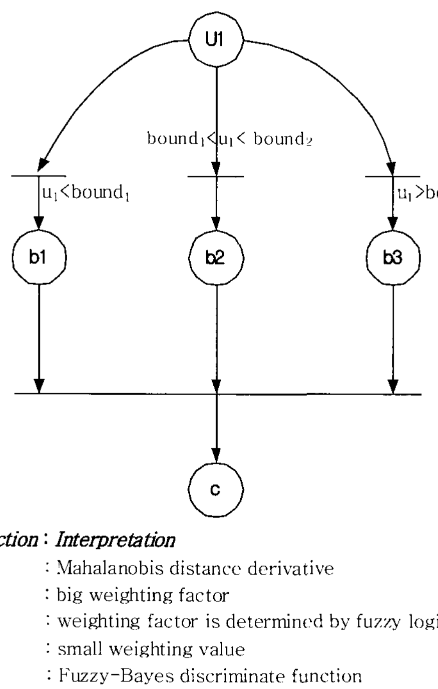

Fig. 1. The classification algorithm of the Fuzzy-Bayes classifier.

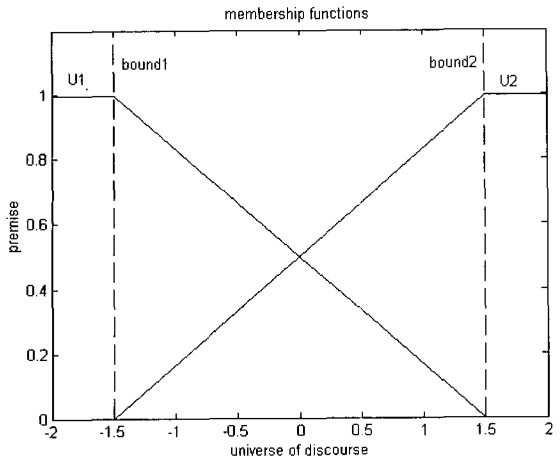

Fig. 2.The Fuzzy membership functions μ_1 and μ_2.

$a_{i,0} + a_{i,1}(u_1)^2 + \cdots + a_{i,n}(u_n)^2$. Therefore, the weighting factor is obtained by defuzzification

$$f_i = \frac{\sum_{i=1}^{R} b_i \mu_i}{\sum_{i=1}^{R} \mu_i}. \tag{7}$$

In this paper, we consider the R=2 case, and μ_i is defined in (8)

$$\mu_i(u_1, u_2, \ldots, u_n) = \mu_{A_1^j}(u_1) * \mu_{A_2^k}(u_2) * \cdots * \mu_{A_n^l}(u_n). \tag{8}$$

The $\mu_i(u_1, u_2, \ldots, u_n)$ presents the certainty that the premise of rule i matches the input information, u_1, when we use singleton fuzzification [7]. Therefore, (7) is represented in (9),

$$f_i = \frac{\mu_1 b_1 + \mu_2 b_2}{\mu_1 + \mu_2}. \tag{9}$$

If $u_1(t) < bound_1$ then $\mu_1 = 1$, and $\mu_2 = 0$, and if $u_1(t) > bound_2$ then $\mu_1 = 0$, and $\mu_2 = 1$. In between $bound_1 \le u_1(t) \le bound_2$, the output f_i is an interpolation amid the two lines μ_1 and μ_2. The fuzzy membership functions are shown in Fig. 2.

3. BLDC MOTOR FAULT DIAGNOSIS SYSTEM

3.1. System configuration

Fig. 3 shows the BLDC motor fault diagnosis system. The system consists of a FDI-master, smart network board, and RS-485 network. The smart network board acquires bridge current and motor speed. The acquired information is transmitted to the FDI-master using the RS-485 communication channel. By design of periodic and deterministic protocol, a real-time fault diagnosis system can be implemented. Figure 4 shows a picture of the test apparatus.

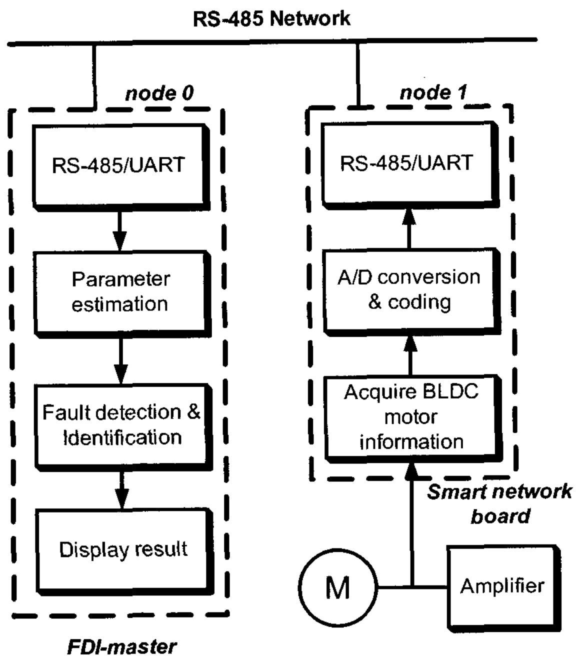

Fig. 3. The BLDC motor fault diagnosis scheme.

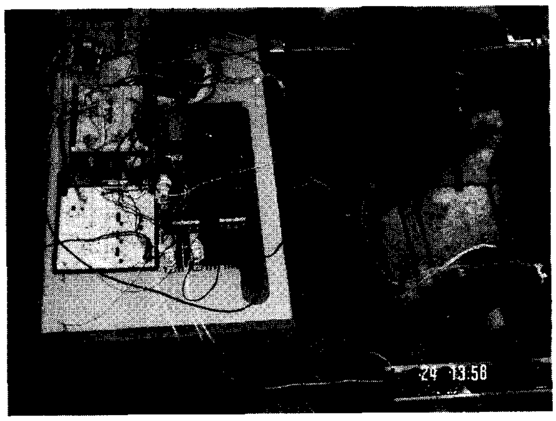

Fig. 4. The BLDC motor fault diagnosis apparatus picture.

3.2. Model-based fault detection

In the diagnosis system, the BLDC motor fault detection model, which is presented by Moseler *et al.* [3,8,9], and least square algorithm are used for model-based fault detection. The model is presented as follows:

$$\bar{v} = \frac{2}{3}(R_1 + R_2 + R_3)\bar{i}(t) + \frac{2}{3}(K_{e1} + K_{e2} + K_{e3})\omega_r(t), \tag{10}$$

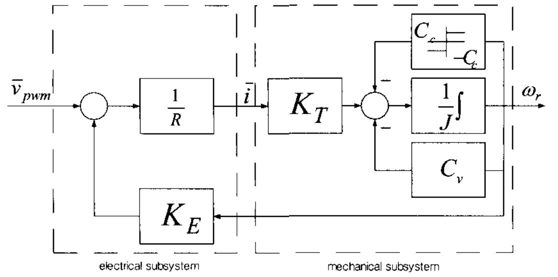

Fig. 5. Block diagram of the BLDC motor fault detection model.

where $\bar{v}(t) = v_{pwm}(t)$ ($v_{pwm}(t)=pwm(t)\cdot V_{supply}$, $pwm(t) \in [0,1]$), R_i is the resistance and K_{ei} ($i=1, 2, 3$) is the back-EMF constant of each coil. Substituting $2/3\cdot(R_1 + R_2 + R_3)$ with R and $2/3\cdot(k_{e1} + k_{e2} + k_{e3})$ with K_E, leads to the equation

$$\bar{v}(t) = R\bar{i}(t) + K_E\omega_r(t). \tag{11}$$

The average phase current $\bar{i}$ can be driven from the bridge current by considering the power balance

$$v_b \cdot i_b(t) = v_{pwm}(t)\cdot \bar{i}(t) = pwm(t)\cdot v_b \cdot \bar{i}, \tag{12}$$

where v_b and i_b denote bridge supply voltage and bridge current. Hence,

$$\bar{i}(t) = i_b(t)/pwm(t). \tag{13}$$

Fig. 5 presents the block diagram of the model, where K_T is torque constant and J denotes the inertia of the rotor. The $c_c \cdot \mathrm{sgn}(\omega_r(t))$ is coulomb friction, and $c_v\omega_r(t)$ is viscose friction.

The quantitative knowledge, the mathematical model of a system, is useful in the detection of a fault. If the system is presented with the mathematical model, we can estimate model parameters based on input and output signals ($u(t)$ and $y(t)$). The least square algorithm is a very simple and robust means of estimating parameters [10].

Perhaps the most basic relationship between the input and output is the linear difference equation:

$$y(t) = -a_1 y(t-1) - \ldots - a_n y(t-n) + b_1 u(t-1) + \ldots + b_m u(t-m). \tag{14}$$

For more compact notation we introduce the vectors:

$$\theta = [a_1 \ \ldots \ a_n \ b_1 \ \ldots \ b_m]^T, \tag{15}$$

$$\varphi(t) = [-y(t-1) \ \ldots \ -y(t-n) \ u(t-1) \ \ldots \ u(t-m)]^T. \tag{16}$$

With these, (14) can be rewritten as

$$y(t) = \varphi^T(t)\theta. \tag{17}$$

The least square algorithm is presented as

$$\hat{\theta}_N = \left[\sum_{t=1}^{N}\varphi(t)\varphi^T(t)\right]^{-1}\sum_{t=1}^{N}\varphi(t)y(t). \tag{18}$$

(18) can be restated as the recursive least square equation (19) to (21)

$$\hat{\theta}(t) = \hat{\theta}(t-1) + L(t)\left[y(t) - \varphi^T(t)\hat{\theta}(t-1)\right], \tag{19}$$

$$L(t) = \frac{P(t-1)\varphi(t)}{\lambda(t) + \varphi^T(t)P(t-1)\varphi(t)}, \tag{20}$$

$$P(t) = \frac{1}{\lambda(t)}\left[P(t-1) - \frac{P(t-1)\varphi(t)\varphi^T(t)P(t-1)}{\lambda(t) + \varphi^T(t)P(t-1)\varphi(t)}\right], \tag{21}$$

where $L(t)$, prefilter allows extra freedom in dealing with non-momentary properties of the prediction errors. In order to let the parameter estimation to follow changing in the system, a forgetting factor λ, which means that older values of $u(t)$ and $y(t)$ do not have as much weight as the newer values, is used. The forgetting factor λ is normally chosen between 0.95 and 1 [11].

4. EXPERIMENTAL STUDIES

The Fuzzy-Bayes isolator is designed for the POWERTEC, L42ALA1100700000 BLDC motor fault diagnosis. The nominal motor parameters are listed in Table 1, where R and K_E are calculated using (22)-(23),

$$R = 2/3\cdot(R_1 + R_2 + R_3) = 2.14\ \Omega, \tag{22}$$

$$K_E = 2/3\cdot(k_{e1} + k_{e2} + k_{e3}) = 0.04\ \text{V/rpm}. \tag{23}$$

In the experiments, three fault types are considered.

Table 1. The nominal BLDC motor parameters.

Parameter	Node 1
resistance, R_1	1.07 Ω
inductance, L_1	6 mH
back-EMF constant, K_{ei}	0.02 V/rpm
torque constant, K_T	0.175 Nm/A
number of pole pairs	4
resistance, R	2.14 Ω
back-EMF constant, K_E	0.04 V/rpm

Table 2. The three fault types and injection methods.

Fault No.	Fault type	Fault injection method
1	fault-free	none
2	increase of R_l	add resistance of 2 Ω
3	more increase of R_l	add resistance of 4 Ω

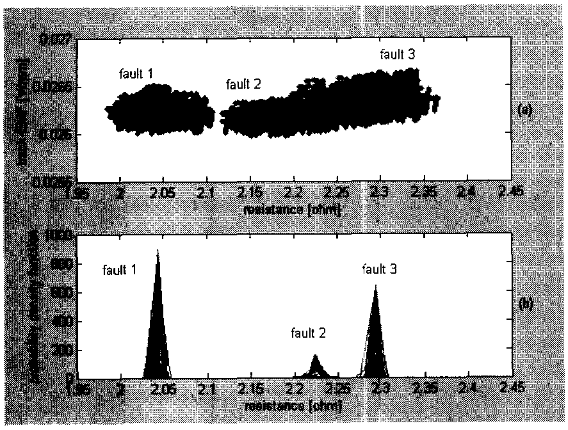

Fig. 6. The scatter diagram of three fault classes (a), and class-conditional probability density (b).

Table 3. The probability knowledge of each fault class.

Fault No.	R [Ω]		K_E [V/rpm]	
	Mean [μ]	Variance [σ^2]	Mean [μ]	Variance [σ^2]
1	2.0435	4.4703e-4	0.0262	6.5171e-9
2	2.2245	0.0025	0.0262	8.2656e-9
3	2.2939	6.2362e-4	0.0264	8.0887e-9

Fault number 1 is the fault-free condition, and faults 2 and 3 are related with resistance variation. An overload is the most significant fault of the motor and is expressed as a heat. The motor coil resistance is changed with the heat. If the coil temperature changes from 20℃ to 100℃, the coil resistance increases by about 30%. The overheating reduces the motor winding life [12]. Therefore, assumed faults are practical. The three fault types and fault injection methods are listed in Table 2.

In the experiments, it is assumed that the three fault classes contain normal class-conditional probability density, and same prior probability. To design the Bayes isolator, the mean and variance of each class are calculated using 30000 training data. Fig. 6 shows the class scatter diagram, and class-conditional probability densities. The mean and variance are listed in Table 3.

To estimate motor parameters, the pseudo-random binary signal (PRBS) input is designed with a 5-cell shift register. Therefore, the maximum period length $M=2^5-1=31$ is obtained. The system input and output signals are plotted in Fig. 7.

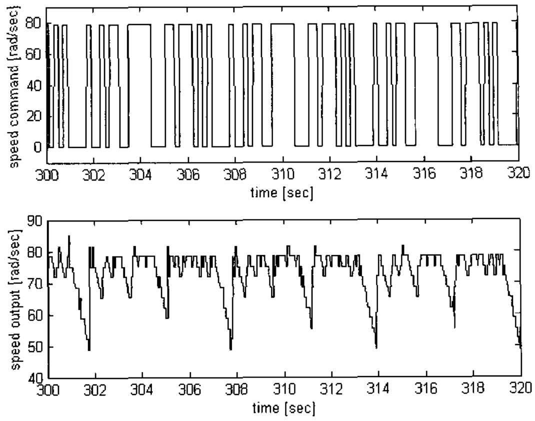

Fig. 7. The system input (speed command) and output (speed output) signal.

The Mahalanobis distance derivative, (24), is selected as the input of the fuzzy inference logic.

$$u_1(t) = (Mahalanobis\ distance(i) - Mahalanobis\ distance(i-1))\ /\ frame\ time. \quad (24)$$

To guarantee a constant frame time, function b_i is defined with constant maximum and minimum values, (25), which use only the necessary calculation time,

$$b_i = [err_{\min}, err_{\max}] = [1.5, -1.5]. \quad (25)$$

The designed two fault diagnosis methods, the Bayes classifier and the Fuzzy-Bayes classifier, are compared by two experiments. The first experiment is the fault isolation experiment. For this experiment, the BLDC motor starts rotating with the occurrence of a fault. Then the designed fault diagnosis scheme isolates the fault. The second experiment is the fault diagnosis experiment. The BLDC motor is derived with a fault-free condition. Some time passed before the fault is injected. The fault diagnosis scheme monitors system condition.

This first set of experiments are divided into two experiments. One is fault 1, and fault 2 isolation experiment. The other is fault 2, and fault 3 isolation experiment. Fig. 6 shows that fault 1 and fault 2 are independent of each other, and fault 2 and fault 3 are highly coupled with each other. In the experiments, a predefined fault is injected before diagnosis is initiated. The estimated resistances for the fault detection are shown in Fig. 8. In the figure, each data is composed of 100000 samples.

Firstly, Fig. 8(a) data is applied to an input of the Bayes fault isolator. The fault isolation result is shown in Fig. 9(a).

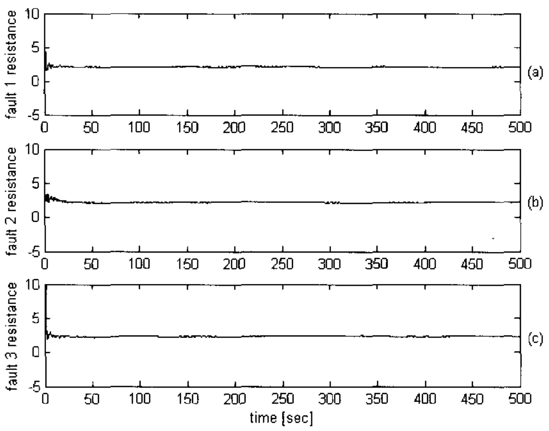

Fig. 8. The estimated resistance, when the three faults are injected: (a) fault 1 resistance, (b) fault 2 resistance, (c) fault 3 resistance.

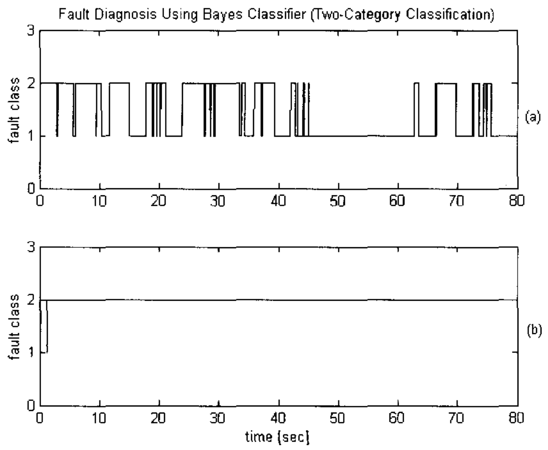

Fig. 9. The fault 1, and fault 2 isolation results using the Bayes isolator: (a) input is fault 1 data, (b) input is fault 2 data.

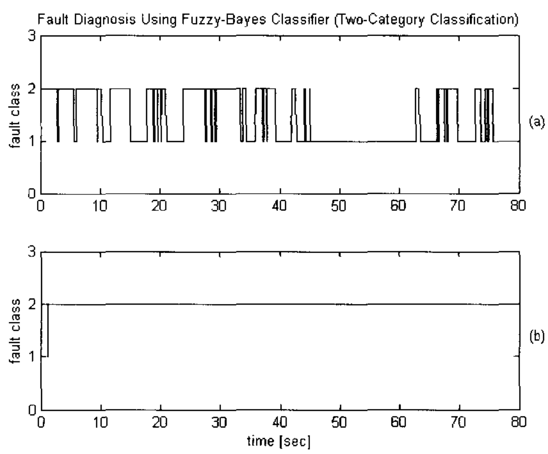

Fig. 10. The fault 1 and fault 2 isolation results using the Fuzzy-Bayes isolator: (a) input is fault 1 data, (b) input is fault 2 data.

In the ideal case, the fault isolation result must indicate fault 1. In the figure, fault 2 indicating data is the error. After that, Fig 8(b) data is applied, and its result is plotted in Fig. 9(b). The Fig. 8(a), and (b) data are also applied to the Fuzzy-Bayes classifier. The fault isolation result of the Fuzzy-Bayes isolator is depicted in Fig. 10. The results are listed in Table 4, and Table 5.

Table 4. The fault isolation result of the Bayes classifier: fault 1 and 2 classification cases.

Input data	Correct diagnosis data		Error data	
	Sample numbers [samples]	Recognition rate [%]	Sample numbers [samples]	Error rate [%]
Fault 1	39052	78.104	10948	21.896
Fault 2	49502	99.004	498	0.996
Total	88554	88.554	11446	11.446

Table 5. The fault isolation result of the Fuzzy-Bayes classifier: fault 1 and 2 classification cases.

Input data	Correct diagnosis data		Error data	
	Sample numbers [samples]	Recognition rate [%]	Sample numbers [samples]	Error rate [%]
Fault 1	39977	79.954	10023	20.0466
Fault 2	49455	98.910	545	1.09
Total	89432	89.432	10568	10.568

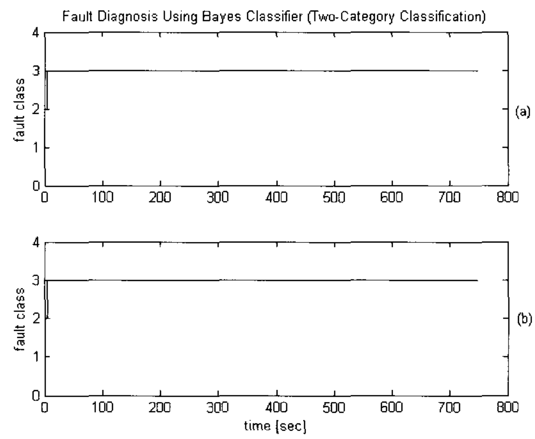

Fig. 11. The fault 2, and fault 3 diagnosis results using the Bayes classifier: (a) input is fault 2 data, (b) input is fault 3 data.

The first experiment results indicate that the Fuzzy-Bayes isolator improves fault isolation rate by 0.878%, and reduces error rate by 0.878% more than the Bayes isolator.

Secondly, Fig. 8(b), and Fig. 8(c) are used as an input of the two fault isolators. The Fig. 6 scatter diagram shows that faults 2 and 3 are highly coupled, therefore isolation will be difficult. The isolation results are depicted in Figs. 11 and 12 and listed in Table 6 and Table 7. In the results, the Fuzzy-Bayes isolator increases isolation rate by 0.065%, and reduces error rate by 0.047% more than the Bayes isolator.

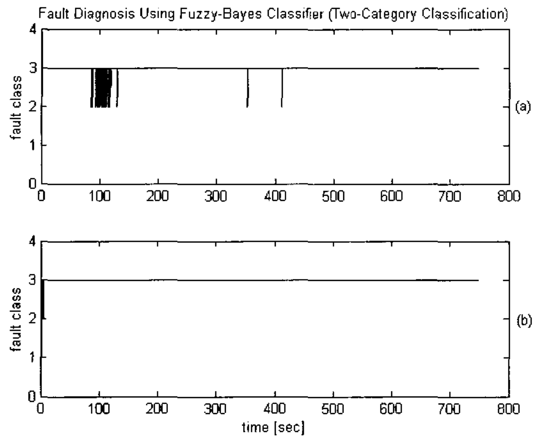

Fig. 12. The fault 2, and fault 3 diagnosis results using the Fuzzy-Bayes classifier: (a) input is fault 2 data, (b) input is fault 3 data.

Table 6. The fault diagnosis result of the Bayes classifier: fault 2 and 3 classification cases.

Input data	Correct diagnosis data		Error data	
	Sample numbers [samples]	Recogni -tion rate [%]	Sample numbers [samples]	Error rate [%]
Fault 2	498	0.996	49502	99.004
Fault 3	49988	99.976	12	0.024
Total	50468	50.468	49514	49.514

Table 7. The fault diagnosis result of the Fuzzy-Bayes classifier: fault 2 and 3 classification cases.

Input data	Correct diagnosis data		Error data	
	Sample numbers [samples]	Recogni -tion rate [%]	Sample numbers [samples]	Error rate [%]
Fault 2	545	1.09	49455	98.91
Fault 3	49988	99.976	12	0.024
Total	50533	50.533	49467	49.467

In the second experiment, fault diagnosis is performed under fault inject condition. The BLDC motor starts with a fault free condition, fault number 1. After 750 seconds pass, fault 2 is injected. The fault diagnosis results of the Bayes classifier and Fuzzy-Bayes classifier are depicted in Figs. 13 and 14. The two figures have two transition regions, which are related with the forgetting factor. In the experiments, the feature data is estimated with a 0.9999 forgetting factor, and it gives 150 seconds, 10000 samples as transition time.

The chattering area in transition region 1 of Fig. 13 is about 135 seconds, and that of Fig. 14 is about 120 seconds. They are the initial time transition regions. After injection of a fault, the transition region 2

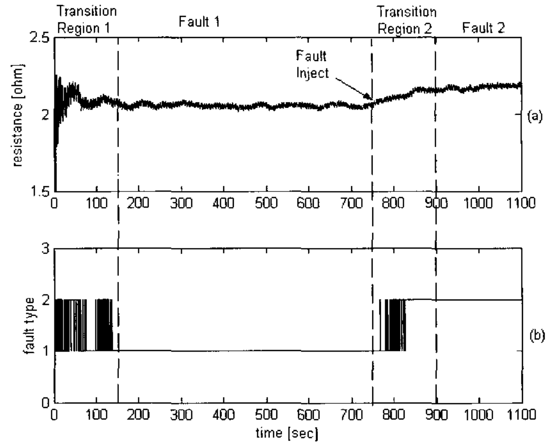

Fig. 13. The fault diagnosis results of the Bayes classifier under fault injection condition: (a) estimated feature data, and (b) fault diagnosis result.

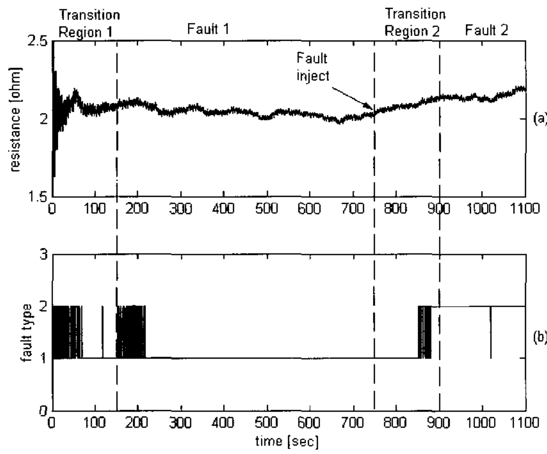

Fig. 14. The fault diagnosis results of the Fuzzy-Bayes classifier under fault injection condition: (a) estimated feature data, and (b) fault diagnosis result.

appears. Transition region 2 has about 66.7 seconds of chattering area in Fig. 13.

In Fig. 14, chattering area is reduced to about 33.3 seconds by the Fuzzy-Bayes classifier. These results show that the Fuzzy-Bayes classifier has an advantage in the transition region. The fault type implies the condition of the current system. Because the chattering is the undetermined condition, reducing chattering is important for fault diagnosis.

To verify performance of the Fuzzy-Bayes classifier, we define three motor resistance variation faults, and conduct two experiments. The defined fault 1 and fault 2 have independent probability characteristics. But, that of fault 2 and fault 3 is highly coupled.

In the first experiment, the fault 1 and fault 2 isolation experiments, results show that the Fuzzy-Bayes isolator improves fault isolation rate by 0.878%, and reduces error rate by 0.878% more than the result of the Bayes isolator. In the fault 2 and fault 3 isolation experiments, the Fuzzy-Bayes isolator improves isolation rate by 0.065%, and reduces of error rate by 0.047% more than the Bayes isolator. Because the experiment is conducted using static data, the performance of the Fuzzy-Bayes isolator is slightly improved.

In the second experiment, the fault diagnosis experiment, results show that the Fuzzy-Bayes isolator can reduce the transition region chattering that is occurred when initial time and fault are injected. In this experiment the chattering is reduced by about half that of the Bayes isolator.

5. CONCLUSIONS

This paper proposes the Fuzzy-Bayes classifier, designed as a fault isolation technique for the BLDC motor fault diagnosis system. It is composed of the Bayes isolator and weighting factor, which is determined by fuzzy inference logic. For the experiments, the Mahalanobis distance derivative is used as an input of the fuzzy inference logic, and mapped according to weighting factor. Therefore, the weighing factor reflects the feature data dynamics. The Fuzzy-Bayes isolator shows improved fault isolation performance over the Bayes isolator. The two experiment results support it. From the experiment results, we can conclude that the proposed Fuzzy-Bayes isolator improves the fault diagnosis performance more significantly than the Bayes isolator. Because the weighting factor reflects the feature data dynamics, the Fuzzy-Bayes isolator can reduce transition region chattering.

REFERENCES

[1] T. G. Park, *Fault Detection and Isolation Schemes Using State Observers and Parity Equations*, Ph.D. thesis, Dankook Univ., 1998.

[2] X.-Q. Liu, H.-Y. Zhang, J. Liu, and J. Yang, "Fault detection and diagnosis of permanent-magnet DC motor based on parameter estimation and neural network," *IEEE Trans. on Industrial Electronics*, vol. 47, no. 5, pp. 1021-1030, October 2000.

[3] O. Moseler and R. Isermann, "Application of model-based fault detection to a brushless DC motor," *IEEE Trans. on Industrial Electronics*, vol. 47, no. 5, pp. 1015-1020, October 2000.

[4] O. Nørretranders, *Fault Diagnosis Using Parameter Estimation and Supervised Classification Techniques*, Intelligent Systems Laboratory Heriot-Watt University, 1997.

[5] S. H. Suh, and K. J. Woo, "Serial communication-based fault diagnosis of a BLDC motor using Bayes classifier," *International Journal of Control, Automation, and Systems*, vol. 1, no. 3, pp. 308-313, September 2003.

[6] R. O. Duda, P. E. Hart, and D. G. Stork, *Pattern Classification*, John Wiley & Sons, Inc., 2001.

[7] K. M. Passino and S. Yurkovich, *Fuzzy Control*, Addison-Wesley, 1998.

[8] O. Moseler and R. Isermann, "Model-based fault detection for a brushless DC motor using parameter estimation," *IECON*, pp. 1956-1960, 1998.

[9] O. Moseler, D. Juričić, A. Rakar, and N. Müller, "Model-based fault diagnosis of an actuator system driven by the brushless DC motor," *Proc. of the American Control Conference*, pp. 3779-3783, 1999.

[10] L. Ljung, *System Identification Theory for the User*, Prentice-Hall, 1999.

[11] J.-W. Seok, K.-S. Choi, J.-S. Lee, and S.-W. Cho, "An improved new RLS algorithm with forgetting factor of Erlang function for system identification," *Journal of Control, Automation and Systems Engineering*, vol. 5, no. 4, pp. 394-402, May 1999.

[12] I. L. Kosow, *Electronic Machinery and Transformers*, Prentice-Hall, 1991.

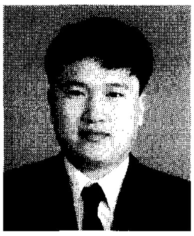

Suhk-Hoon Suh received his B.S., M.S., and Ph.D. degrees in Electronic Engineering from Dankook University in 1990, 1992, and 2003, respectively. His research interests include dynamic system fault diagnosis, control network application, embedded real-time system, and motor control.